Aspects of the magnetic structure of $TmCu_2$

1992 J. Phys.: Condens. Matter 4 8773

(http://iopscience.iop.org/0953-8984/4/45/012)

J. Phys.: Condens. Matter 4 (1992) 8773–8782. Printed in the UK

Aspects of the magnetic structure of $TmCu_2$

M Heidelmann†, B Lebech‡, Z Smetana§ and M Loewenhaupt†

† Institut für Festkörperforschung der KFA Jülich, Postbox 1913, W-5170 Jülich, Federal Republic of Germany

‡ Department of Solid State Physics, Risø National Laboratory, Postbox 49, DK-4000 Roskilde, Denmark

§ Department of Metal Physics, Charles University, De Karlovu 5, 12116 Prague 2, Czechoslovakia

Received 1 May 1992, in final form 17 July 1992

Abstract. An investigation has been made, using neutron diffraction, of the temperature dependence of the complex magnetic behaviour of $TmCu_2$ in its ordered states. The samples were mainly powdered, but some aspects have also been tested by single-crystal measurements. $TmCu_2$ shows at least three different antiferromagnetic structures in its ordered state. Within these phases, the magnetic structures show a strong ferromagnetic coupling of the moments of next-neighbour Tm atoms in the *b* direction. The low-temperature structure (AFI) is composed by the first two odd harmonics of a propagation vector $(2\pi/8)a^*$, where the strongest magnetic intensity is caused by the third harmonic. The first phase transition occurs close to 3.1 K. The phase that develops here is a mixture of two structures (AFII). At a temperature close to 4.7 K a third phase (AFIII) appears. The propagation vectors of the structures AFII and AFIII are at least two dimensional. All these structures may be described as sinusoidally modulated with magnetic moments lying in the direction of the easy magnetic axis (*b*), except for one of the components of AFII, where it is necessary to invoke a component perpendicular to the *b* axis.

1. Introduction

The intermetallic compounds RCu_2 (where R is a rare earth) show a rich variety of different magnetic structures. During the last ten years many experimental investigations have been performed to get more insight into the complex magnetic behaviour of these structures, but a lot of questions are still open, and some structural aspects were only be described by models that resulted in large reliability factors [1].

$TmCu_2$ is one member of the isostructural RCu_2 series. All these compounds crystallize in the orthorhombic structure of $CeCu_2$ (see figure 1). It is well known from measurements of the thermodynamic bulk properties of $TmCu_2$ (specific heat [2], thermal expansion [3], magnetization [4], and so on) that in a zero magnetic field $TmCu_2$ exhibits at least two phase transitions below T_N.

In the ordered state the arrangement of the magnetic moments of the RCu_2 class is determined by at least two types of interactions of the 4f electron shells of the rare earth ions with the surrounding ions and the band electrons. Firstly, the crystal-field anisotropy may be responsible for the preferred plane or direction of the magnetic moment orientation. Secondly, the exchange coupling of the well localized 4f electron shells has to be indirect. This coupling is probably mediated via the

0953-8984/92/458773+10$07.50

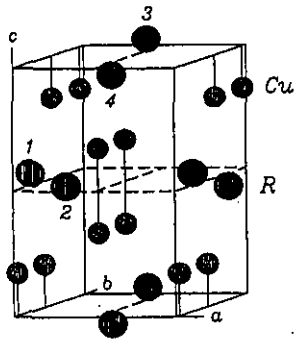

Figure 1. Crystallographic unit cell of the orthorhombic RCu_2 compounds. The four Tm atoms are labelled 1, 2, 3 and 4.

conduction electrons. Such an RKKY-like exchange interaction may be responsible for the observed long-range ordering of the magnetic moments. At low temperatures dipole–dipole interactions may also be important. In the special case of magnetic crystal-field singlets (i.e. the case of even J) the magnetic moments are induced by the exchange coupling of the crystal-field states [5].

The purpose of this article is to present the results of a neutron scattering investigation of the complex magnetic behaviour of $TmCu_2$ in its ordered states, and to propose further studies which may lead to a more complete understanding of the magnetic structure of $TmCu_2$.

2. Sample and measurements

The present neutron diffraction studies were done mainly using a polycrystalline sample. A single crystal was only used to test some conclusions drawn from the powder measurements.

The powder sample was prepared by melting a stoichiometric mixture of 4N Tm and 5N Cu in a cold copper crucible under argon pressure. During this procedure a small part of Tm vaporized because of the relatively high vapour pressure of Tm at its melting point ($\approx 10^2$ Torr). The material obtained was then powdered mechanically and annealed at $\approx 750°$C in a high vacuum for four days. After that the powder was characterized by x-ray (Debye–Scherrer) analysis and it was found that it contained more than 98% $TmCu_2$ by weight. By means of x-ray analysis the lattice parameters at room temperature were determined to be $a = (4.267 \pm 0.002)$ Å, $b = (6.713 \pm 0.006)$ Å and $c = (7.247 \pm 0.004)$ Å. These parameters are in agreement with those of [4].

The single crystal was a small grain from a polycrystalline sample, identified by x-ray analysis. The preparation procedure of the crystal involved arbitrary aspects, because a straightforward growing process using standard methods (Czochralsky, Bridgman) has so far been unsuccessful.

The neutron diffraction measurements were performed at the research reactor DR3 at Risø National Laboratory, Denmark. The instruments were cold-neutron source triple-axis spectrometers (TAS1, TAS6) operating in the elastic mode with pyrolytic graphite monochromators and analysers. The measurements were done using either 20 meV or 5 meV neutron energies. In the first case, we used the (004) reflection from the monochromator and the (002) reflection from the analyser to select

only the 2 Å (20 meV) neutrons from the white beam incident to the monochromator. In the second case we used the (002) reflection from both the monochromator and analyser and inserted a cooled Be filter after the monochromator in order to select only the 4 Å neutrons from the beam emerging from the monochromator. In both cases the analyser ensures that we observe only elastic scattering with a resolution improved signal-to-noise ratio.

3. Results

3.1. Crystalline structure

The nuclear structure of the powder sample was measured by neutron diffraction. From a refinement of the nuclear diffraction pattern at a neutron incident energy of 20 meV the lattice parameter of the orthorhombic cell were found to be $a = (4.28 \pm 0.02)$ Å, $b = (6.64 \pm 0.02)$ Å and $c = (7.20 \pm 0.02)$ Å at $T \approx 20$ K. Within experimental accuracy these parameters are temperature independent in the temperature range $1.4\,\mathrm{K} < T < 20\,\mathrm{K}$. The positions of the Tm atoms in the unit cell are given by

$$r_1 = (0, \tfrac{1}{4}, z) \qquad r_2 = (0, \tfrac{3}{4}, 1-z) \qquad r_3 = (\tfrac{1}{2}, \tfrac{3}{4}, \tfrac{3}{2}-z) \qquad r_4 = (\tfrac{1}{2}, \tfrac{1}{4}, \tfrac{1}{2}+z)$$

where the z parameter is very close to 0.55.

3.2. Magnetic structure

In the magnetic structure the magnetic moments are confined to the nuclear positions of the Tm atoms, i.e.

$$r_{iN} = r_i + R_N \qquad \text{where} \quad R_N = n_1 a + n_2 b + n_3 c.$$

The magnetic structure factor can then be written in the form

$$F(k) = f(k) \sum_{i,N} m_{iN} e^{ik \cdot r_{iN}}$$

where k is the scattering vector, $f(k)$ is the magnetic form factor and m_{iN} is the magnetic moment of the Tm atom at the position r_{iN}, where (i, N) runs over all the Tm atoms in the magnetic unit cell. The magnetic moments can be written in their Fourier representations:

$$m_{iN} = \sum_q m_i(q) e^{iq \cdot r_{iN}}.$$

At the positions of the interference maxima the magnetic structure factor has the form

$$F(k) = f(k) \sum_i m_i(q) e^{iG_{hkl} \cdot r_i} \qquad \text{with} \quad k = G_{hkl} \pm q$$

where q is the propagation vector of the Fourier component $m_i(q)$ and G_{hkl} is the reciprocal lattice vector of the nuclear unit cell:

$$G_{hkl} = 2\pi(ha^* + kb^* + lc^*).$$

In the special case of the RCu_2 compounds the magnetic structure factor is

$$F(k) = f(k)\left[(m_1 + Dm_3)e^{2\pi i(k/4+zl)} + (m_2 + Dm_4)e^{-2\pi i(k/4+zl)}\right]$$

with

$$m_i = m_i(q) \qquad D = e^{i\pi(h+k+l)}.$$

3.2.1. Low-temperature structure (AFI). In the temperature range $1.4\,\mathrm{K} < T < 3.1\,\mathrm{K}$ the magnetic structure can be described by the two propagation vectors

$$P = 2\pi(0.125 \pm 0.005)a^* \qquad Q = 2\pi(0.375 \pm 0.005)a^*.$$

These two vectors may also be written in the form $P = 2\pi\frac{1}{8}a^*$ and $Q = 2\pi\frac{3}{8}a^*$. Therefore this structure may be described as a composition of two magnetic Fourier components, the first and the third harmonic of a commensurate structure with a unit cell eight times the unit cell of the nuclear structure in the a direction. To find the underlying orientations of the magnetic moments, two kinds of magnetic superstructures were considered: sinousoidally modulated and helical structures. With a sinousoidally modulated structure it was possible to fit the neutron diffraction pattern satisfactorily at $T = 2.5\,\mathrm{K}$. The fitting procedure was performed as follows. The positions and intensities of the magnetic Bragg reflections were found by a trial and error procedure which finally led to the assumed model. After that the widths of the individual Bragg reflections were fitted by a least-square fit in order to estimate the decreasing resolution of the instrument with increasing scattering angle.

Using the smoothed dependence of width against scattering vector the full diffraction pattern, assuming Gaussian lineshapes, was then fitted to the assumed model for the magnetic structure. The magnetic moments are oriented along the b direction. The sinousoidally modulated moments can be written in the form

$$m_{iN} = m_i \cos(q \cdot r_{iN} + \phi_i).$$

In this case the structurally related part of the magnetic intensity is

$$I(k) \sim \tfrac{1}{4}\sin^2(k,m)\left|\sum_i m_i e^{i(G_{hkl}\cdot r_i \pm \phi_i)}\right|^2$$

with

$$k = G_{hkl} \pm q.$$

Here (k,m) is the angle between the scattering vector and the magnetic moment direction. The propagation vector q takes the values P and Q. The phases ϕ_i have been determined to be $\phi_1 = \phi_2 = \frac{3\pi}{8}$ and $\phi_3 = \phi_4 = -\frac{\pi}{2}$ for the third harmonic and $\phi_1 = \phi_2 = \phi_3 = \phi_4 = 0$ for the first harmonic. Thus the moments of the nearest-neighbour Tm atoms (along the b axis) have the same direction and the same length for both Fourier components. The four amplitudes m_i are equal. The amplitude m_i of the magnetic moment can be determined by comparing the magnetic intensity with the nuclear intensity of the (011) nuclear Bragg reflection. For the third harmonic the value is close to $4\mu_B$. The relation between $m_i(Q)$ and $m_i(P)$ is $m_i(P) \approx 0.32 m_i(Q)$, which is very close to $m_i(P) = \frac{1}{3}m_i(Q)$.

This model has been verified by single-crystal measurements at 1.4 K with respect to the positions of the magnetic reflections in the reciprocal space. Therefore other possibilities for describing the positions of the Bragg peaks found in the powder can be excluded.

Figure 2(a) and (b) show the fit of the neutron diffraction profile at 5 meV incident neutron energy. The theoretical curve is simply an addition of the calculated intensities of both Fourier components. The proposed structure is shown in figure 3.

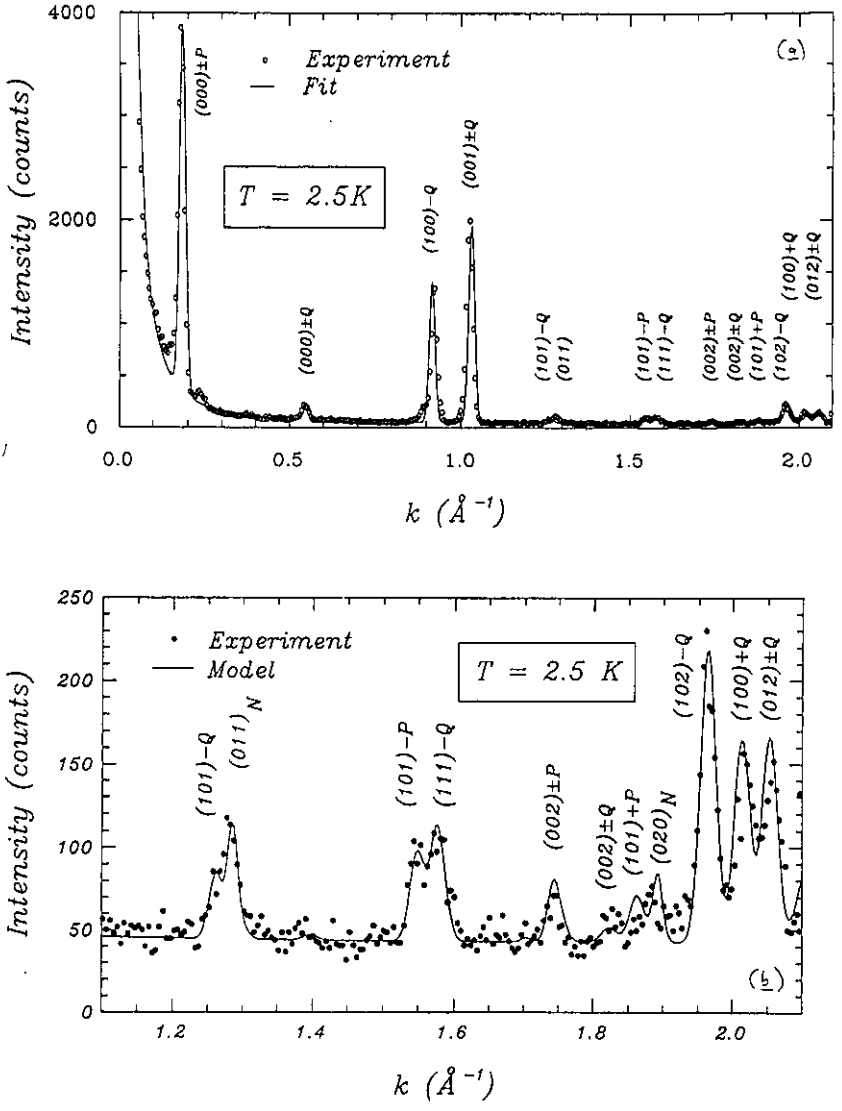

Figure 2. (*a*) Fit of the model AFI to the neutron diffraction powder data at 5 meV incident neutron energy. Only one of the Bragg peaks with different (hkl) and the same length of the scattering vector is indexed. The propagation vectors labelled $\boldsymbol{Q}$ and $\boldsymbol{P}$ refer to the third and first order satellites, respectively (see text). The background curve follows from a background constant multiplied by the scattering vector dependent geometrical Lorentz factor of the sample. (*b*) Inset to (*a*).

3.2.2. Higher temperature structures. When the sample temperature exceeded a value close to $T = 3.1$ K two effects were observed. The first effect was a splitting of the magnetic Bragg peak at the position $(000) \pm \boldsymbol{P}$ into two peaks, see figure 4. The second effect was the appearance of pronounced shoulders close to the other magnetic peaks of the low-temperature structure, see figure 5.

Before determining the change of the structure with temperature two aspects needed to be examined. These aspects are, first, the time, τ, it takes for the sample

Figure 3. 3D model of the magnetic moment distribution of the two Fourier components of AFI. The moments of the component $(\frac{1}{8}, 0, 0)$ are drawn too long (by a factor three) in comparison with those of $(\frac{3}{8}, 0, 0)$. The true magnetic structure is obtained as the vector sum of the $\boldsymbol{Q}$ component and $\frac{1}{3}$ of the $\boldsymbol{P}$ component.

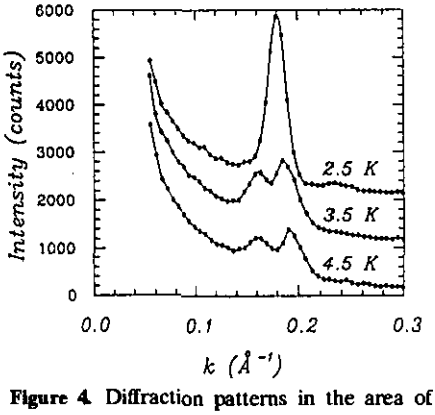

Figure 4. Diffraction patterns in the area of small scattering vectors at different temperatures. The splitting of the intense peak close to 0.18 $Å^{-1}$ into two peaks close to 0.16 $Å^{-1}$ and 0.19 $Å^{-1}$ is remarkable. (The shift of consecutive patterns is 1000 units on the intensity scale.)

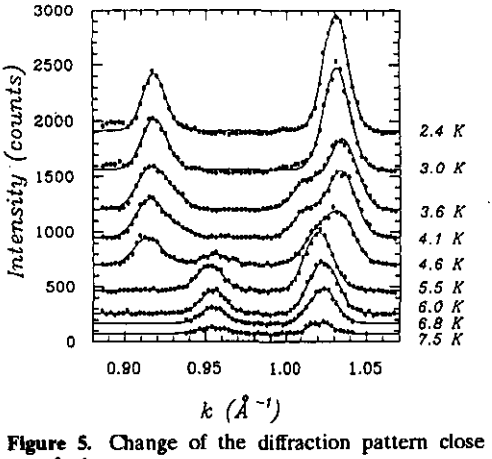

Figure 5. Change of the diffraction pattern close to 1 $Å^{-1}$ with temperature (selected temperatures). The lines are the single line fits which lead to the results represented in figures 6 and 7.

to reach thermal equilibrium after the change of temperature and, second, whether it showed signs of thermal hysteresis. Fortunately τ was short, of the order of seconds, and thermal equilibrium was easily achieved.

The thermal hysteresis needed to be checked in order to ensure that the experimental results were not influenced by the way in which the sample was thermally cycled. Concerning the possibility of thermal hysteresis, the most intense magnetic Bragg peaks around 1 $Å^{-1}$ were scanned with respect to the temperature by cooling from the paramagnetic region down to 2 K and after that by heating from 2 K to above T_N. Within the limits of the experimental error there was no difference between these intensities.

After these tests, the magnetic Bragg peaks with scattering vectors around 1 $Å^{-1}$ were followed as function of temperature, and the resulting peak profiles were fitted to Gaussians with equal half widths, see figure 5. The temperature dependencies of the peak positions and intensities are shown in figure 6 and figure 7.

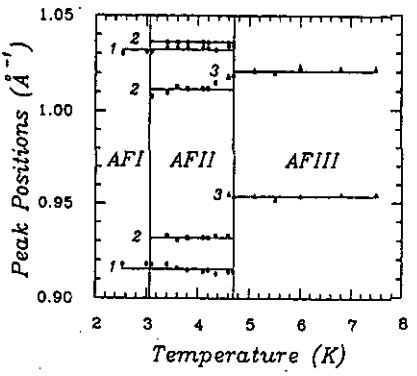

Figure 6. Temperature dependence of the positions of selected magnetic Bragg reflections in the reciprocal space, measured at 5 meV incident neutron energy. The positions of AFI and AFIII are observed directly in the diffraction patterns. Those of AFII are derived from the diffraction patterns after fitting to the proposed model structure. The numbers 1, 2, 3 refer to the three different third harmonic wavevectors $\boldsymbol{Q}_1 = 2\pi(\frac{3}{8}, 0, 0)$, $\boldsymbol{Q}_2 = 2\pi(0.367, 0, 0.018)$ and $\boldsymbol{Q}_3 = 2\pi(0.355, 0.127, 0)$. Here the lower group of peaks correspond to $(100) - \boldsymbol{Q}_i$ and the upper group of peaks to $(001) \pm \boldsymbol{Q}_i$.

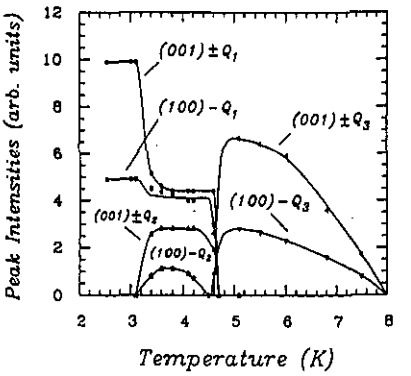

Figure 7. Temperature dependence of the intensities of selected magnetic Bragg reflections in the reciprocal space, measured at 5 meV neutron incident energy. The intensities of AFI and AFIII are observed directly in the diffraction patterns. Those of AFII are derived from the diffraction patterns after fitting to the proposed model structure. This figure corresponds to figure 6.

3.2.3. High-temperature structure (AFIII). We first discuss the structure AFIII, which develops in the temperature region $4.7\,\mathrm{K} < T < T_N$.

It is not possible to find a *one*-dimensional propagation vector that describes AFIII properly. There is only one two-dimensional vector close to the propagation vector of AFI which is able to account correctly for the measured peak positions: $\boldsymbol{Q}_3 = 2\pi(0.355\boldsymbol{a}^* + 0.127\boldsymbol{b}^*)$. With this propagation vector, and a sinousoidally modulated structure with magnetic moments in the b direction, it is possible to fit the diffraction data, for instance at $T = 5.2\,\mathrm{K}$, see figure 8. The phases in this model are $\phi_1 = \phi_2 = \frac{\pi}{2}$ and $\phi_3 = \phi_4 = -\frac{\pi}{2}$. The amplitudes m_i of the modulated structure are equal and close to a value of $3\mu_B$.

Unfortunately the weak Bragg reflections indexed in figure 8 are to close to the statistics of the experiment, so that they are not resolved here.

3.2.4. Intermediate structure (AFII). The magnetic structure AFII develops in the temperature region $3.1\,\mathrm{K} < T < 4.7\,\mathrm{K}$. This structure AFII contains components whose magnetic Bragg peaks were not resolved with the present instrumental resolution. At least two different propagations coexist. One component is very close to the propagation vector $\boldsymbol{Q}$ of AFI and the other is at least two dimensional.

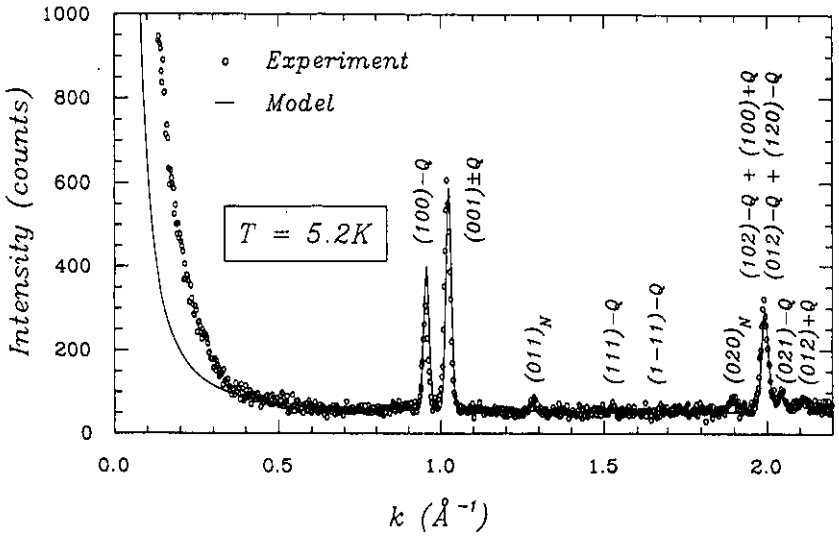

Figure 8. Fit of the model AFIII to the neutron diffraction powder data at 5 meV incident neutron energy. Only one of the Bragg peaks with different (hkl) and the same length of the scattering vector is indexed. The line of the background follows from a background constant multiplied with the scattering vector dependent geometrical Lorentz factor of the sample. Here $\boldsymbol{Q} = \boldsymbol{Q}_3$, see text.

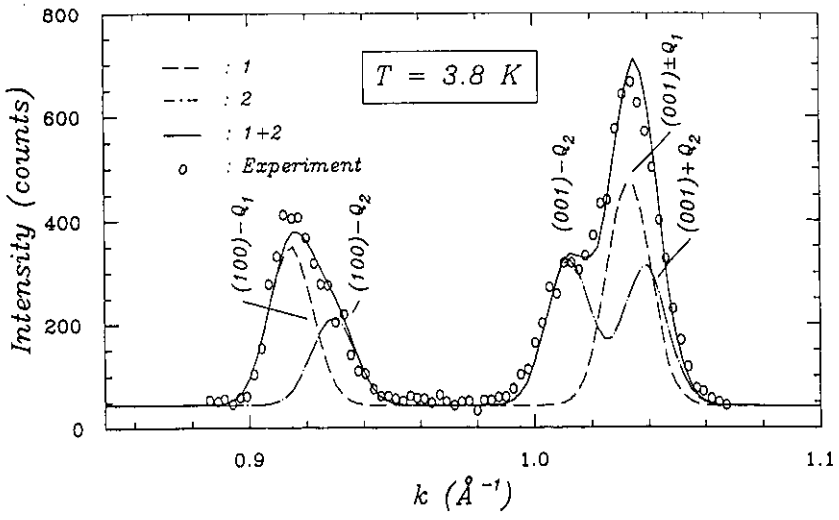

Figure 9. Fit of the structure model for AFII to the Bragg reflections of the powdered sample around a scattering vector of 1 $Å^{-1}$ at 5 meV incident neutron energy.

The simplest vector close to $\boldsymbol{Q}$ that describes the scattering pattern properly is $\boldsymbol{Q}_2 = 2\pi(0.367\boldsymbol{a}^* + 0.018\boldsymbol{c}^*)$. This structure is also sinousoidally modulated with the same phases ϕ_i as those found in AFIII. The magnetic moment of this second component is not along the high-symmetry $\boldsymbol{b}$ direction, but close to $\boldsymbol{a} + 0.5\boldsymbol{b}$. A fit to the experimental data of this model, with equal m_i, is shown in figure 9.

4. Discussion

In the present investigation, there is only one region ($T < 3.1$ K) where the magnetic structure model has been tested by single-crystal measurements with respect to the positions of the propagation vectors in reciprocal space. The powder pattern agrees well with the proposed model for the magnetic structure. This last statement is also true in AFIII, except for the fact that there is unresolved magnetic scattering intensity below scattering vectors of 0.3 $Å^{-1}$.

The most difficult temperature region is that of AFII. The measured lines here are not yet resolved, so the proposed magnetic structure model includes a certain amount of doubt. Also the two Bragg reflections around a scattering vector of 0.18 $Å^{-1}$ cannot be explained analogously to the two harmonics of phase AFI.

Concerning the Néel temperature (T_N) there is a large discrepancy between the Néel temperature obtained from bulk data and the Néel temperature obtained from neutron diffraction in this work. In [1, 2, 4] T_N was found to be close to 6.3 K. In the neutron investigation T_N was found to be close to 8 K. The authors have no reasonable explanation for this discrepancy. The trivial explanation of an erroneous temperature calibration had to be excluded after a recalibration of the thermometer, which was carried out shortly after the collection of the diffraction data. A possible temperature gradient may also be ruled out, both because the sample was kept in an He-exchange gas and because of the rather instantaneous response of the sample to changes in temperature (see subsection 3.2.2).

From bulk data [2] four phase-transition temperatures have been proposed. The specific heat shows small steps at 3.3 K and 3.9 K, a pronounced peak at 4.3 K and a pronounced step at 6.3 K. However, from the neutron diffraction data there is no evidence that the transition at 3.9 K exists.

In the case of AFI and AFIII only one magnetic moment component in the b direction is necessary to describe the observed structure well. This is in agreement with the crystal-field anisotropy [1] and the magnetization measurements.

The fact, that the magnetic moment is not the full free-ion moment of the Tm^{3+} ions ($7\mu_B$) is also in agreement with the results of the crystal-field anisotropy. In orthorhombic systems the crystal-field multiplet of the 4f electrons has no remaining degeneracy. In fact, the ground state and the first excited state of the Tm^{3+} ion in the paramagnetic area are singlets [1]. So the magnetic moments are purely induced by exchange coupling or by an external magnetic field. Because of the fact that the two lowest levels are well separated from the rest of the crystal-field multiplet [1] they show Ising-like behaviour. The moment at each Tm site is either + or $-\mu$, where the size of μ depends on the local exchange of the wavefunctions of this moment.

The next step in the progress of understanding the magnetic structure of $TmCu_2$ will be to check the positions of the propagation vectors of AFII and AFIII in reciprocal space by single-crystal measurements, and the establishment of the magnetic phase diagram (B, T).

References

[1] Šima V, Diviš M, Svoboda P, Smetana Z, Zajac Š and Bischof J 1989 *J. Phys.: Condens. Matter* **1** 10153–63

[2] Smetana Z, Šima V, Bischof J, Svoboda P, Zajac Š, Havela L and Andreev A V 1986 *J. Phys. F: Met. Phys.* **16** L201–4

[3] Šima V, Smetana Z, Diviš M, Svoboda P, Zajac Š, Bischof J, Lebech B and Kayzel F 1988 *J. Physique Coll.* 12 C8 49
[4] Svoboda P, Smetana Z and Andreev A V 1989 *Phys. Status Solidi* a 111 285
[5] Bleaney B 1963 *Proc. R. Soc.* A 276 19